

Published in final edited form as:

*Circulation*. 2009 January 27; 119(3): 408–416. doi:10.1161/CIRCULATIONAHA.108.822072.

## Ventricular phosphodiesterase 5 expression is increased in patients with advanced heart failure and contributes to adverse ventricular remodeling after myocardial infarction in mice

Peter Pokreisz, PhD<sup>a,d</sup>, Sara Vandewijngaert, MS<sup>a</sup>, Virginie Bito, PhD<sup>d</sup>, An Van den Bergh, PhD<sup>c</sup>, Ilse Lenaerts, MS<sup>d</sup>, Cornelius Busch, MD<sup>g</sup>, Glenn Marsboom, PhD<sup>a</sup>, Olivier Gheysens, MD<sup>e</sup>, Pieter Vermeersch, MD<sup>a</sup>, Liesbeth Biesmans, MS<sup>d</sup>, Xiaoshun Liu, MD, PhD<sup>a</sup>, Hilde Gillijns, BS<sup>a</sup>, Marijke Pellens, BS<sup>a</sup>, Alfons Van Lommel, PhD<sup>f</sup>, Emmanuel Buys, PhD<sup>g</sup>, Luc Schoonjans, PhD<sup>a</sup>, Johan Vanhaecke, MD, PhD<sup>b</sup>, Erik Verbeken, MD, PhD<sup>f</sup>, Karin Sipido, MD, PhD<sup>d</sup>, Paul Herijgers, MD, PhD<sup>c</sup>, Kenneth D. Bloch, MD<sup>g</sup>, and Stefan Janssens, MD, PhD<sup>a,b</sup>

<sup>a</sup>Vesalius Research Center (VIB3); KU Leuven, Leuven, Belgium

<sup>b</sup>Division of Clinical Cardiology, KU Leuven, Leuven, Belgium

<sup>c</sup>Experimental Cardiac Surgery, KU Leuven, Leuven, Belgium

<sup>d</sup>Experimental Cardiology, KU Leuven, Leuven, Belgium

<sup>e</sup>Imaging and Cardiovascular Dynamics, Department of Cardiovascular Medicine, KU Leuven, Leuven, Belgium

<sup>f</sup>Department of Medical Diagnostic Sciences, KU Leuven, Leuven, Belgium

<sup>g</sup>Cardiovascular Research Center and Department of Anesthesia and Critical Care, Massachusetts General Hospital and Harvard Medical School, Boston, MA, USA

### Abstract

**Background**—Ventricular expression of phosphodiesterase-5 (PDE5), an enzyme responsible for cGMP catabolism, is increased in human right ventricular hypertrophy, but its role in left ventricular (LV) failure remains incompletely understood. We therefore measured LV PDE5 expression in patients with advanced systolic heart failure and characterized LV remodeling after myocardial infarction (MI) in transgenic mice with cardiomyocyte-specific over-expression of PDE5 (PDE5-TG).

**Methods and Results**—Immunoblot and immunohistochemistry techniques revealed that PDE5 expression was greater in explanted LVs from patients with dilated and ischemic cardiomyopathy than in control hearts. To evaluate the impact of increased ventricular PDE5 levels on cardiac function, PDE5-TG mice were generated. Confocal and immunoelectron microscopy revealed increased PDE5 expression in cardiomyocytes predominantly localized to Z-bands. At baseline, myocardial cGMP levels, cell shortening and calcium handling in isolated cardiomyocytes, and LV hemodynamic measurements were similar in PDE5-TG and wild-type littermates (WT). Ten days after MI, LV cGMP levels increased to a greater extent in WT than PDE5-TG ( $P < 0.05$ ). Ten weeks after MI, LV end-systolic and -diastolic volumes were larger in

**Address for correspondence:** Stefan Janssens, MD, PhD, Division of Clinical Cardiology and Vesalius Research Center, University of Leuven, Campus Gasthuisberg, 49 Herestraat, B-3000 Leuven, Belgium, Tel: +32-16-345775 ; Fax: +32-16-345990, stefan.janssens@med.kuleuven.be.

**Conflict of Interest Disclosures.**

None.

PDE5-TG than in WT ( $57\pm 5$  vs  $39\pm 4$  and  $65\pm 6$  vs  $48\pm 4$   $\mu\text{L}$ , respectively,  $P<0.01$  for both). LV systolic and diastolic dysfunction was more marked in PDE5-TG than WT associated with enhanced hypertrophy and reduced contractile function in isolated cardiomyocytes from remote myocardium.

**Conclusions**—Increased PDE5 expression predisposes mice to adverse LV remodeling after MI. Increased myocardial PDE5 expression in patients with advanced cardiomyopathy may contribute to the development of heart failure and represents an important therapeutic target.

### Keywords

phosphodiesterase-5; cyclic guanosine monophosphate (cGMP); myocardial infarction; heart failure

### Introduction

In the heart, cyclic adenosine and guanosine monophosphates (cAMP and cGMP) are important second messenger molecules controlled by tightly-regulated, and compartmentalized synthesis and degradation processes. cAMP and cGMP have often opposing roles in cardiovascular homeostasis as many of the inotropic and chronotropic effects of  $\alpha$ -adrenergic stimulation in the mammalian heart are mediated by cAMP, while cGMP opposes these effects via activation of its intracellular target protein kinase G (PKG).<sup>1–3</sup> Cardiac cGMP synthesis is stimulated by activation of soluble guanylate cyclase (sGC) by nitric oxide (NO) and by the binding of natriuretic peptides to their receptors (NPR-1 and  $-2$ ).<sup>4–6</sup> cGMP is catabolized by phosphodiesterases (PDEs), many of which are compartmentalized in cardiomyocytes.<sup>2, 3, 7</sup> Of the 11 different known PDE isoenzymes, PDE5, PDE6, and PDE9 degrade cGMP specifically, whereas PDE1–3, and PDE 10–11 can hydrolyze both cAMP and cGMP.<sup>8</sup> Cardiac cAMP hydrolysis, under normal conditions, is predominantly controlled by PDE3 and PDE4, and PDE4-knockout mice develop progressive cardiomyopathy.<sup>9, 10</sup> Increased cGMP concentrations can modulate cardiomyocyte contractility by inhibiting PDE3-mediated cAMP hydrolysis or stimulating PDE2-mediated cAMP hydrolysis, but PDE2 represents a minor part of cAMP hydrolysis in cardiomyocytes.<sup>2, 8, 11, 12</sup>

The role of PDE5 in regulating smooth muscle tone in the systemic and pulmonary vasculature has long been recognized.<sup>13</sup> Because PDE5 expression in the heart under normal physiological conditions is low, the importance of PDE5 has only recently begun to be appreciated in cardiac disease when perturbations in NO and natriuretic peptide signaling occur.<sup>11, 14, 15</sup> For example, Takimoto and colleagues reported that transverse aortic constriction increased LV PDE5 expression and that treatment with sildenafil, a specific PDE5 inhibitor, prevented the development of LV hypertrophy and reversed already established LV remodeling.<sup>16</sup> Recently, Nagendran et al. reported that PDE5 expression was increased in right ventricular (RV) biopsies of patients with RV hypertrophy and pulmonary hypertension.<sup>17</sup> However, it remained to be determined whether PDE5 expression is increased in the LVs of patients with cardiomyopathy and whether increased PDE5 expression contributes to adverse LV remodeling or protects against it.

In the present study, we measured PDE5 expression in LVs of patients with end-stage cardiomyopathy and observed that PDE5 expression was markedly greater in LV tissues from these patients than in unused donor LV tissues. To evaluate the impact of increased ventricular PDE5 expression on cardiac function, we characterized LV structure and function in wild-type mice and mice with cardiomyocyte-specific over-expression of PDE5

at baseline and after MI. We report that increased ventricular PDE5 expression does not affect baseline cardiac function but predisposes mice to adverse LV remodeling after MI.

## Methods

### Human cardiac samples

Cardiac tissue samples were obtained from patients with ischemic and dilated cardiomyopathy (IDM, DCM) who were referred for cardiac transplantation to Gasthuisberg University Hospital (University of Leuven, Belgium) and Massachusetts General Hospital (Harvard University, Boston). Unused LV tissues from donors without documented prior cardiac disease were studied as controls. PDE5 expression and collagen deposition were analyzed using immunohistochemical and immunoblot techniques (n=10 cardiomyopathy patients and 5 control hearts, for details see supplemental methods).

### Experimental Animals

The bovine PDE5 cDNA (Genbank L16545, revised Apr11, 1996), kindly provided by J. Corbin, was ligated into a plasmid containing the  $\beta$ -myosin heavy chain promoter.<sup>18</sup> A restriction fragment, containing the full expression cassette was microinjected into FVB mouse eggs (Charles River Laboratories, Wilmington, MA). Oocytes were implanted into a pseudopregnant Swiss foster mother, and offspring were screened using PCR to confirm successful transgene integration. Transgenic founders were backcrossed for 5 generations onto a C57BL/6 background. Wild-type littermates served as controls in all experiments.

### Measurement of PDE5 expression using immunoblot, immunohistochemical, and immunoelectron microscopy techniques

Levels of PDE5 protein in mouse LV were measured using immunoblot and immunohistochemical techniques and a rabbit anti-PDE5 polyclonal antibody. Subcellular localization of PDE5 was ascertained in cardiomyocytes isolated from wild-type and PDE5-TG mice (supplemental methods). Cardiomyocytes were stained with rabbit polyclonal PDE5 antiserum and a murine monoclonal antibody recognizing desmin (#M0760, DAKO, Denmark). Bound primary antibodies were revealed using Alexa488- and Alexa568-labeled goat anti-rabbit and anti-mouse polyclonal antibodies, respectively. Nuclei were stained using TOPRO-3 (Invitrogen, Merelbeke, Belgium). Cardiomyocytes were examined using confocal laser scanning microscopy (LSM510, Zeiss, Germany).

For immunoelectron microscopy studies, 1- $\mu$ m thick sections from resin-embedded hearts were stained using a gold-labeled goat anti-rabbit antibody (supplemental methods).

### Left ventricular PDE activity, and cyclic nucleotide levels

cGMP-hydrolyzing PDE enzyme activity in hearts from WT and PDE5-TG was measured in the presence and absence of sildenafil (2  $\mu$ M) using a [8-<sup>3</sup>H]cGMP conversion assay following a modification of the method described by Turko et al. (supplemental methods).<sup>19</sup> Sildenafil-inhibitable cGMP catabolism was measured over a wide range of substrate concentrations (0.06–100  $\mu$ M), and  $K_m$  (cGMP concentration at which activity was half-maximal) was determined.

Cyclic nucleotide concentrations were measured in lyophilized extracts prepared from LVs at baseline and at 10 days and 10 weeks after MI using an enzyme-linked immunoassay (supplemental methods).

### Quantitative PCR analysis

Expression of genes encoding proteins involved in cGMP metabolism was measured using quantitative reverse-transcriptase PCR (qPCR) analysis on ventricular samples obtained from hearts of WT and PDE5-TG using SYBR<sup>®</sup> Green (Applied Biosystems). Specific primers recognizing sequences of cDNAs encoding murine PDE2, PDE3, PDE5, soluble guanylate cyclase subunits (sGC<sub>1</sub> and sGC<sub>2</sub>), cGMP-dependent protein kinase (PKG-I), NPR-1, and NPR-2 were used (Supplemental Table S1). Transcript levels were normalized to levels of mRNAs encoding hypoxanthine phospho-ribosyl transferase (HPRT) or 18S ribosomal RNA.

### Contractility and calcium studies in isolated cardiomyocytes

Cardiomyocytes were isolated from WT and PDE5-TG at baseline and at 10 weeks after MI, as previously described, and examined in a perfusion chamber mounted on the stage of an inverted microscope (Nikon Diaphot).<sup>20</sup> Cell length and width were determined in a random sample of 40 cardiomyocytes per heart with 3–5 animals examined per group and condition. Cell shortening during field stimulation at 0.5, 1, 2, and 4 Hz was measured with a video edge-detector (Crescent Electronics, Sandy, UT). After stabilization at 1 Hz, the effect of  $\beta$ -adrenergic stimulation (isoproterenol, 50 nM) on cell shortening was recorded in the presence or absence of PDE5 inhibitor II (30 nM, 2-Butyl-5-(4-methoxyphenyl)-5,6,11,11a-tetrahydro-1H-imidazo[1',5':1,6]pyrido[3,4-b]indole-1,3(2H)-dione, #524714, Calbiochem). Percent cell shortening (CS%) was calculated as the ratio of twitch amplitude (L) to diastolic length (L<sub>0</sub>), and time to peak shortening (TTP) and half-time of relaxation (RT<sub>50</sub>) were determined. L-type calcium currents (I<sub>CaL</sub>) and intracellular calcium concentrations were measured using the whole-cell ruptured patch-clamp technique (supplemental methods).<sup>20</sup>

### Hemodynamic measurements at baseline and after MI

MI was induced in 2–4 month old PDE5-TG and WT by permanent ligation of the LAD coronary artery, as described previously.<sup>21</sup>

For invasive, closed chest hemodynamic measurements, mice were anesthetized using urethane and  $\alpha$ -chloralose (1200 and 50 mg/g body weight, IP) and mechanically ventilated. Instantaneous LV pressures and volumes with and without preload reduction were recorded in unoperated mice (WT n=16 and PDE5-TG n=11) and in mice 10 weeks after MI (n=15, for both genotypes) using a 1.4-F Millar SPR830 pressure-conductance catheter (Millar Instruments, TX) as described previously.<sup>22</sup> We also performed separate hemodynamic measurements in unoperated 44-week old mice of both genotypes (n=10). Indices of systolic and diastolic function were calculated including ejection fraction (EF), preload-recrutable-stroke work (PRSW), arterial elastance (E<sub>a</sub>), preload-adjusted maximal power (PAMP), and the time constant of isovolumic relaxation ( $\tau$ ). The response to  $\beta$ -adrenergic stimulation was studied in additional unoperated mice and in mice 10 weeks after MI during infusion of dobutamine (1, 3, and 10 ng/g/min, n=7 for each genotype and condition).

### Histological analysis of LV remodeling after MI

After completion of hemodynamic measurements 10 weeks after MI, LVs were weighed, and cardiomyocyte width was measured in the remote, noninfarcted area of laminin-stained 5- $\mu$ m-thick LV sections. To assess the degree of fibrosis in the LV, the area of collagen deposition was traced on Sirius red-stained sections using polarized light and spectral thresholding (supplemental methods).

Infarct size was determined in additional WT and PDE5-TG 3 days after LAD ligation on consecutive Sirius red-stained sections encompassing the entire LV free wall, according to the midline infarct length method validated by Takagawa et al.<sup>23</sup>

### Statistical Analysis

All data are expressed as mean±SEM unless indicated otherwise. Differences between groups were determined using Student t-test, ANOVA, or 2-way ANOVA for repeated measurements, where indicated. When applicable, significant differences were further analyzed using Bonferroni and Student-Newman-Keuls post hoc tests. A value of  $P<0.05$  was considered significant.

The authors had full access to and take full responsibility for the integrity of the data. All authors have read and agree to the manuscript as written.

## Results

### Increased PDE5 expression in LV tissues from patients with endstage heart failure

In LVs from patients without cardiac disease, PDE5 expression was minimal in cardiomyocytes, as well as in myocardial extracts (Figure 1, A and J), but PDE5 was readily detectable in vascular smooth muscle (Figure 1 A, inset). In contrast, we detected markedly increased PDE5 immunoreactivity in cardiomyocytes from DCM and ICM patients (Figure 1, D and G) and in myocardial extracts from DCM patients (Figure 1J). Densitometric analysis confirmed an almost 5-fold increase in PDE5 expression levels (Figure 1K, \* $P<0.01$ ). In heart failure patients, the PDE5 expression pattern was non-uniform, and PDE5 immunoreactivity was scattered between areas of fibrosis, as indicated by the Sirius red-stain (Figure 1, F and I).

### PDE5 localizes to sarcomeric Z-bands and is abundantly expressed in cardiomyocytes from PDE5-TG

PDE5 immunoreactivity was much more prominent in LV tissue and in cardiomyocytes from PDE5-TG (Figure 2 A-B) than in WT mice (Figure 2 C-D). The intensity and distribution of recombinant PDE5 was comparable in newborn and in 2- to 6-month old PDE5-TG mice (data not shown). Immunoblot analysis revealed abundant 98-kDa PDE5 protein in hearts of PDE5-TG mice: PDE5 expression was almost 9-fold greater in PDE5-TG than in WT LV extracts (Figure 2, E-F,  $P=0.001$ ).

To investigate the intracellular localization of PDE5 in WT and PDE5-TG, confocal laser scanning microscopy was performed on isolated cardiomyocytes using fluorescently-labeled antibodies against PDE5 (green, Figure 3, A and D) and desmin (red, Figure 3, B and E). In WT cardiomyocytes, low levels of PDE5 immunoreactivity were predominantly localized around Z-bands. In contrast, high PDE5 levels were detected in PDE5-TG cardiomyocytes. The merged images (yellow, Figure 3, C and F) and the immunoelectron microscopy analysis (Supplemental Figure S1) confirmed that recombinant PDE5 were predominantly localized to sarcomeric Z-bands.

### Enhanced PDE5 enzymatic activity does not affect myocardial cyclic GMP levels at baseline or expression of cGMP-metabolizing enzymes

Sildenafil-inhibitable cGMP hydrolysis, a measure of PDE5 enzyme activity, was 10-fold greater in PDE5-TG than WT LV extracts. The  $K_m$  for PDE5 in transgenic mice ( $4.9\pm 0.8$   $\mu\text{M}$ ) did not differ from values reported for purified bovine PDE5 (Supplemental Figure S2).<sup>24</sup> At baseline, concentrations of cGMP in LV extracts were very low and did not differ between PDE5-TG and WT ( $0.013\pm 0.004$  versus  $0.013\pm 0.008$  pmol/mg protein,

respectively,  $n=8$  for both). Moreover, baseline cAMP nucleotide levels were similar in LV extracts from PDE5-TG and WT ( $1.76\pm 0.08$  and  $1.58\pm 0.04$  pmol/mg protein,  $n=12$  for both).

Cardiomyocyte-specific overexpression of PDE5 did not affect LV expression of endogenous PDE isoforms (including PDE2, PDE3, and PDE5), PKG-I, sGC subunits, or natriuretic peptide receptors (WT  $n=9$ , PDE5-TG  $n=10$ ; Supplemental Figure S3).

### **Enhanced PDE5 enzymatic activity does not affect baseline excitation–contraction coupling of isolated cardiomyocytes**

At baseline, contraction amplitude and kinetics were similar in WT and PDE5-TG cardiomyocytes (Figure 4A, mean cell shortening, normalized to resting cell length,  $L/L_0$ , was 7.6% and 7.3%, respectively,  $n_{\text{cells}} > 60$  per genotype). The infusion of isoproterenol increased absolute cell shortening in both genotypes (Figure 4B), while preincubation with PDE5 inhibitors modestly but significantly reduced isoproterenol-mediated fractional cell shortening (Figure 4C). The amplitude and voltage-dependence of calcium currents were similar in both genotypes (Figure 4D), as were calcium transients at varying stimulation frequencies (Supplemental Figure S4).

### **PDE5 overexpression does not affect baseline cardiac function**

Baseline LV systolic function (SW, PAMP) and relaxation ( ) did not differ between PDE5-TG and WT (Table 1). In both genotypes, infusion of sildenafil reduced LV afterload by ~10% and attenuated the dobutamine-induced rise in PRSW, a load-independent index of contractile function (data not shown).

### **PDE5 overexpression predisposes mice to adverse LV remodeling after MI**

Three days after LAD ligation, infarct size as a percentage of LV was similar in WT and PDE5-TG ( $36\pm 5\%$  versus  $35\pm 9\%$ , Supplemental Figure S5). However, 10 weeks after MI, LV end-systolic and end-diastolic volumes (ESV and EDV) were larger in PDE5-TG than in WT (Figure 5, A and B). In PDE5-TG, LVEF and PRSW were less than in WT (Figure 5, C and D). Diastolic function was also impaired to a greater extent in PDE5-TG, as indicated by the more marked prolongation of (Table 1).

Myocardial contractile reserve, 10 weeks after MI, was evaluated using graded beta-adrenergic stimulation with dobutamine. Infusion of dobutamine increased the heart rate in a dose-dependent manner similarly in both genotypes (Figure 5E). In contrast, the ability of dobutamine to increase PRSW after MI was impaired in PDE5-TG suggesting a genotype-dependent reduction in myocardial contractile reserve (Figure 5F). Overall survival rates at 10 weeks after MI were not different in WT and PDE5-TG, although mortality was higher in male compared to female mice, irrespective of genotype.

Whereas at baseline the heart-to-body weight ratio (HW/BW) did not differ between genotypes, at 10 weeks after MI, HW/BW was greater in PDE5-TG than in WT ( $P < 0.05$ , Table 2). Ten weeks after MI, cardiomyocyte width in remote myocardium was greater in PDE5-TG than in WT ( $16.6\pm 0.1$  versus  $15.1\pm 0.3$   $\mu\text{m}$ ,  $n=7$  for both,  $P < 0.001$ , Figure 6) suggesting greater hypertrophy in PDE5-TG. Deposition of thick, tightly-packed type I collagen fibers and thin, loosely-assembled type III collagen fiber did not differ between genotypes after MI (Table 2).

### **Enhanced PDE5 expression reduces myofilament calcium sensitivity after MI**

To investigate the mechanisms responsible for greater impairment of myocardial contractile function after MI in PDE5-TG, cell shortening and intracellular calcium transients were

studied in cardiomyocytes isolated from WT and PDE5-TG at 10 weeks after MI. Cardiomyocyte length tended to be greater in PDE5-TG than in WT cells ( $198 \pm 22$  versus  $162 \pm 6$   $\mu\text{m}$ ,  $P=0.07$ ,  $n_{\text{cells}} > 120$  in each group). Cell capacitance, a measure of total membrane surface area, was significantly greater in PDE5-TG than in WT cells ( $292 \pm 26$  versus  $200 \pm 9$  pF,  $n_{\text{cells}}=18$  and  $25$ , respectively,  $P < 0.05$ ). The amplitude of cell shortening was decreased in both genotypes after MI, as compared to baseline values, particularly at higher stimulation frequencies (Figure 7A; baseline values  $> 8\%$  shortening, see Supplemental Figure S4). The rates of contraction and relaxation were less in PDE5-TG than in WT cells (Figure 7, B and C). In addition, resting diastolic calcium levels and amplitude of calcium transients were significantly greater at all stimulation frequencies in PDE5-TG cardiomyocytes (Figure 7, D and E), but kinetics were not different from WT (data not shown). Calcium currents and sarcoplasmic reticulum calcium content did not differ between genotypes (data not shown). Increased calcium transients in the presence of slower contractions suggest that myofilament responsiveness to calcium was less in PDE5-TG than in WT cardiomyocytes after MI.

### Enhanced PDE5 enzymatic activity reduces cGMP levels in infarcted hearts

Ten days after MI, myocardial cGMP and cAMP concentrations increased in both genotypes when compared to baseline ( $P < 0.01$  and  $P < 0.05$ , respectively). However, cGMP concentrations increased greater than 10-fold in WT ( $0.17 \pm 0.02$  pmol/mg protein,  $n=7$ ), whereas this increase was attenuated in PDE5-TG ( $0.09 \pm 0.02$  pmol/mg protein,  $n=9$ ,  $P < 0.05$  versus WT). In contrast, the rise in cAMP levels 10 days after MI was not different between WT and PDE5-TG ( $7.79 \pm 2.80$ ,  $n=8$ , versus  $8.99 \pm 1.90$  pmol/mg protein,  $n=9$ , respectively,  $P=0.72$ ). Ten weeks after MI, myocardial cGMP levels were less and were no longer different between genotypes ( $0.06 \pm 0.02$  in WT,  $n=8$ , and  $0.04 \pm 0.03$  pmol/mg protein in PDE5-TG,  $n=7$ ).

### Discussion

In this study, we report that PDE5 is markedly expressed in LVs from patients with end-stage ischemic and dilated cardiomyopathy, while PDE5 expression was barely detectable in hearts from patients without cardiac disease (Figure 1). In patients with CHF, PDE5 immunoreactivity was markedly increased in cardiomyocytes between areas of fibrosis. To investigate whether enhanced expression of PDE in the failing LV was protective or deleterious, we characterized the LV remodeling response to MI in transgenic mice with cardiomyocyte-selective PDE5 over-expression. In cardiomyocytes from PDE5-TG mice, we observed abundant PDE5 expression, with a marked clustering to Z-bands, as confirmed by confocal fluorescence imaging and immunoelectron microscopy. At baseline, total myocardial cGMP levels were very low in PDE-TG and WT. In addition, cardiomyocyte-specific overexpression of PDE5 did not alter cardiac structure or function at baseline and did not affect sarcomere shortening, calcium transients, or peak calcium currents. After MI, however, myocardial cGMP levels increased greater than 10-fold in WT, but this increase was significantly reduced in PDE5-TG. After MI, PDE5 overexpression led to a more marked impairment of LV systolic and diastolic function associated with an inability to mount a contractile response to  $\alpha$ -adrenergic stimulation. Isolated cardiomyocytes from PDE5-TG mice after MI also had impaired contraction and relaxation with reduced myofilament responsiveness to calcium. Taken together, these results suggest cGMP signaling has an important role in limiting the acute stress response after MI and the long-term adverse LV remodeling and functional impairment.

In the mammalian heart, PDE5 is expressed at low levels, and, because of its subcellular localization to Z-bands, it is thought to regulate intracellular cGMP microdomains that modulate beta-adrenergic contractility.<sup>3</sup> Inhibition of PDE5 has little effect on myocardial

cGMP levels at baseline but enhances cGMP concentrations in these microdomains under conditions associated with hemodynamic and neurohumoral stress.<sup>3, 16</sup> Elevated cGMP levels counteract cAMP-mediated inotropic effects of catecholamines in mouse, dog, and human heart<sup>25–28</sup> and pressure-overload-induced hypertrophic remodeling in mouse hearts.<sup>15</sup> Our studies confirm that PDE5 expression levels are very low in normal human hearts and are the first to demonstrate markedly enhanced expression in residual cardiomyocytes of patients with end-stage ischemic or idiopathic dilated cardiomyopathy. Because the role of enhanced PDE5 expression in advanced heart failure is incompletely understood, we generated mice with cardiomyocyte-specific overexpression of PDE5 and studied functional and structural characteristics at baseline and in response to MI.

In PDE5-TG mice, the recombinant protein has the expected Km of bovine PDE5 and is predominantly localized within the cells to Z-bands. At baseline, we did not detect a difference in cardiac cGMP levels between genotypes. Moreover, hemodynamic measurements in intact animals and electrophysiologic studies in isolated cardiomyocytes suggested that overexpression of PDE5 did not affect baseline cardiac function (Figure 4C). This is consistent with limited activation of both soluble and particulate guanylate cyclases under normal physiological circumstances when NO and natriuretic peptides levels are low.<sup>15, 29</sup> In contrast, we observed that MI induces a 10-fold increase in myocardial cGMP levels in WT mice, but that the increase was significantly reduced in PDE5-TG mice. Our experiments do not allow identification of the mechanisms responsible for this increase, which may be related to increased atrial or brain natriuretic peptide production or induction of cardiac NO synthesis after MI.<sup>29, 30</sup> Increased cGMP levels may protect against the acute  $\beta$ -adrenergic stress in the first 10 days after MI and against adverse LV remodeling and hypertrophy in remote myocardium thereafter. Failure to increase myocardial cGMP levels could then account for the greater functional impairment and increased cardiomyocyte hypertrophy in PDE5-TG. Accentuated hypertrophy and impaired function of isolated cardiomyocytes from PDE5-TG further indicate a more profound maladaptive remodeling at the myocyte level.

How does the impaired ability to increase cGMP levels after MI contribute to excess LV dilatation and hypertrophy in transgenic mice? One possibility is that increased cGMP levels reduce MI size and thereby the stimulus to LV remodeling. This is unlikely because MI size 3 days after LAD ligation was similar in both genotypes (Supplemental Figure S5). A second possibility is that increased LV cGMP levels after MI counteract adverse remodeling effects of excessive  $\beta$ -adrenergic signaling induced by hemodynamic and neurohumoral stress. Unopposed catecholamine signaling has been shown to contribute to cardiac dysfunction in paced animals and in heart failure patients deprived of  $\beta$ -blocker therapy.<sup>31</sup> A third possibility is that increased cGMP levels may inhibit cAMP-hydrolysis by PDE3, augmenting LV cAMP levels and contractile function after MI and thereby limiting the stimulus to adverse LV remodeling. Nagendran and colleagues reported that pharmacological PDE5 inhibition increased contractility of RV myocytes by inhibiting PDE3-mediated cAMP catabolism.<sup>17</sup> Finally, increased cGMP levels may counteract adverse LV remodeling after MI via cAMP-independent mechanisms, for instance via PKG-dependent pathways. The observation that the increase in cardiac cAMP levels 10 days after MI did not differ in WT and PDE5-TG mice suggests that increased cardiac cGMP levels protects against adverse LV remodeling via a cAMP-independent mechanism.

We recognize the limitations of our study. First, lifelong myocardial overexpression of the transgene may trigger counter-regulatory or compensatory changes in cyclic nucleotide signaling, despite similar expression of other PDEs and cGMP-generating enzymes (Supplemental Figure S3). In addition, our observations in end-stage heart failure patients do



not permit us to conclusively establish the pathophysiological role for PDE5, which requires further prospective studies.

Our data suggest that PDE5 may have an important role in heart failure and that PDE5 inhibitors may be a valuable new treatment strategy. Initial studies of patients with systolic heart failure and RV dysfunction/pulmonary hypertension suggest that sildenafil can improve exercise tolerance and hemodynamics.<sup>32</sup> Our findings add additional impetus to studies using PDE5 inhibitors to prevent and/or treat adverse LV remodeling.

In summary, PDE5 is markedly upregulated in cardiomyocytes of patients with end-stage heart failure. Cardiac-restricted overexpression of PDE5 does not affect baseline myocardial structure or function, but significantly reduces systolic and diastolic function following MI and exacerbates adverse LV remodeling. These observations identify increased PDE5 expression in the LV as a novel target for heart failure treatment.

## Supplementary Material

Refer to Web version on PubMed Central for supplementary material.

## Acknowledgments

The authors thank Federica del Monte MD, PhD, Thomas MacGillivray MD, and Judith Gwathmey MD for providing myocardial tissue samples from patients.

### Funding Sources

This work was supported by the Fund for Scientific Research-Flanders G.0381.05 (P.H.), EWM-B4361-G.0442.06 (S.J.) and Flemish Institute for Biotechnology (VIB, to S.J.), NIH HL070896 (K.D.B.), Research Fund K.U. Leuven OT/05/55 (P.H.) and GOA/2007/13 (K.S., P.P. S.J.), and European Union LSHM-CT-2005-018833, EUGeneHeart (V.B.). S.J. is a Principal Investigator of VIB and holder of a chair supported by Astra-Zeneca.

## References

1. Houslay MD, Baillie GS, Maurice DH. cAMP-Specific phosphodiesterase-4 enzymes in the cardiovascular system: a molecular toolbox for generating compartmentalized cAMP signaling. *Circ Res.* 2007; 100:950–966. [PubMed: 17431197]
2. Fischmeister R, Castro LR, Abi-Gerges A, Rochais F, Jurevicius J, Leroy J, Vandecasteele G. Compartmentation of cyclic nucleotide signaling in the heart: the role of cyclic nucleotide phosphodiesterases. *Circ Res.* 2006; 99:816–828. [PubMed: 17038651]
3. Takimoto E, Belardi D, Tocchetti CG, Vahebi S, Cormaci G, Ketner EA, Moens AL, Champion HC, Kass DA. Compartmentalization of cardiac beta-adrenergic inotropy modulation by phosphodiesterase type 5. *Circulation.* 2007; 115:2159–2167. [PubMed: 17420342]
4. Tremblay J, Desjardins R, Hum D, Gutkowska J, Hamet P. Biochemistry and physiology of the natriuretic peptide receptor guanylyl cyclases. *Mol Cell Biochem.* 2002; 230:31–47. [PubMed: 11952095]
5. Friebe A, Koesling D. Regulation of nitric oxide-sensitive guanylyl cyclase. *Circ Res.* 2003; 93:96–105. [PubMed: 12881475]
6. Cerra MC, Pellegrino D. Cardiovascular cGMP-generating systems in physiological and pathological conditions. *Curr Med Chem.* 2007; 14:585–599. [PubMed: 17346149]
7. Su J, Scholz PM, Weiss HR. Differential effects of cGMP produced by soluble and particulate guanylyl cyclase on mouse ventricular myocytes. *Exp Biol Med (Maywood).* 2005; 230:242–250. [PubMed: 15792945]
8. Omori K, Kotera J. Overview of PDEs and their regulation. *Circ Res.* 2007; 100:309–327. [PubMed: 17307970]
9. Mongillo M, McSorley T, Evellin S, Sood A, Lissandron V, Terrin A, Huston E, Hannawacker A, Lohse MJ, Pozzan T, Houslay MD, Zaccolo M. Fluorescence resonance energy transfer-based

analysis of cAMP dynamics in live neonatal rat cardiac myocytes reveals distinct functions of compartmentalized phosphodiesterases. *Circ Res.* 2004; 95:67–75. [PubMed: 15178638]

10. Lehnart SE, Wehrens XH, Reiken S, Warriar S, Belevych AE, Harvey RD, Richter W, Jin SL, Conti M, Marks AR. Phosphodiesterase 4D deficiency in the ryanodine-receptor complex promotes heart failure and arrhythmias. *Cell.* 2005; 123:25–35. [PubMed: 16213210]
11. Kass DA, Champion HC, Beavo JA. Phosphodiesterase type 5: expanding roles in cardiovascular regulation. *Circ Res.* 2007; 101:1084–1095. [PubMed: 18040025]
12. Mongillo M, Tocchetti CG, Terrin A, Lissandron V, Cheung YF, Dostmann WR, Pozzan T, Kass DA, Paolocci N, Houslay MD, Zaccolo M. Compartmentalized phosphodiesterase-2 activity blunts beta-adrenergic cardiac inotropy via an NO/cGMP-dependent pathway. *Circ Res.* 2006; 98:226–234. [PubMed: 16357307]
13. Lewis GD, Semigran MJ. Type 5 phosphodiesterase inhibition in heart failure and pulmonary hypertension. *Curr Heart Fail Rep.* 2004; 1:183–189. [PubMed: 16036043]
14. Rybalkin SD, Rybalkina IG, Feil R, Hofmann F, Beavo JA. Regulation of cGMP-specific phosphodiesterase (PDE5) phosphorylation in smooth muscle cells. *J Biol Chem.* 2002; 277:3310–3317. [PubMed: 11723116]
15. Kass DA, Takimoto E, Nagayama T, Champion HC. Phosphodiesterase regulation of nitric oxide signaling. *Cardiovasc Res.* 2007; 75:303–314. [PubMed: 17467673]
16. Takimoto E, Champion HC, Li M, Belardi D, Ren S, Rodriguez ER, Bedja D, Gabrielson KL, Wang Y, Kass DA. Chronic inhibition of cyclic GMP phosphodiesterase 5A prevents and reverses cardiac hypertrophy. *Nat Med.* 2005; 11:214–222. [PubMed: 15665834]
17. Nagendran J, Archer SL, Soliman D, Gurtu V, Moudgil R, Haromy A, St Aubin C, Webster L, Rebecka IM, Ross DB, Light PE, Dyck JR, Michelakis ED. Phosphodiesterase type 5 is highly expressed in the hypertrophied human right ventricle, and acute inhibition of phosphodiesterase type 5 improves contractility. *Circulation.* 2007; 116:238–248. [PubMed: 17606845]
18. Turko IV, Haik TL, McAllister-Lucas LM, Burns F, Francis SH, Corbin JD. Identification of key amino acids in a conserved cGMP-binding site of cGMP-binding phosphodiesterases. A putative NKXnD motif for cGMP binding. *J Biol Chem.* 1996; 271:22240–22244. [PubMed: 8703039]
19. Turko IV, Ballard SA, Francis SH, Corbin JD. Inhibition of cyclic GMP-binding cyclic GMP-specific phosphodiesterase (Type 5) by sildenafil and related compounds. *Mol Pharmacol.* 1999; 56:124–130. [PubMed: 10385692]
20. Antoons G, Ver Heyen M, Raeymaekers L, Vangheluwe P, Wuytack F, Sipido KR. Ca<sup>2+</sup> uptake by the sarcoplasmic reticulum in ventricular myocytes of the SERCA2b/b mouse is impaired at higher Ca<sup>2+</sup> loads only. *Circ Res.* 2003; 92:881–887. [PubMed: 12663488]
21. Janssens S, Pokreisz P, Schoonjans L, Pellens M, Vermeersch P, Tjwa M, Jans P, Scherrer-Crosbie M, Picard MH, Szelid Z, Gillijns H, Van de Werf F, Collen D, Bloch KD. Cardiomyocyte-specific overexpression of nitric oxide synthase 3 improves left ventricular performance and reduces compensatory hypertrophy after myocardial infarction. *Circ Res.* 2004; 94:1256–1262. [PubMed: 15044322]
22. Van den Bergh A, Flameng W, Herijgers P. Parameters of ventricular contractility in mice: influence of load and sensitivity to changes in inotropic state. *Pflugers Arch.* 2008; 455:987–994. [PubMed: 17932685]
23. Takagawa J, Zhang Y, Wong ML, Sievers RE, Kapasi NK, Wang Y, Yeghiazarians Y, Lee RJ, Grossman W, Springer ML. Myocardial infarct size measurement in the mouse chronic infarction model: comparison of area- and length-based approaches. *J Appl Physiol.* 2007; 102:2104–2111. [PubMed: 17347379]
24. Thomas MK, Francis SH, Corbin JD. Characterization of a purified bovine lung cGMP-binding cGMP phosphodiesterase. *J Biol Chem.* 1990; 265:14964–14970. [PubMed: 1697584]
25. Takimoto E, Champion HC, Belardi D, Moslehi J, Mongillo M, Mergia E, Montrose DC, Isoda T, Aufiero K, Zaccolo M, Dostmann WR, Smith CJ, Kass DA. cGMP catabolism by phosphodiesterase 5A regulates cardiac adrenergic stimulation by NOS3-dependent mechanism. *Circ Res.* 2005; 96:100–109. [PubMed: 15576651]

26. Senzaki H, Smith CJ, Juang GJ, Isoda T, Mayer SP, Ohler A, Paolucci N, Tomaselli GF, Hare JM, Kass DA. Cardiac phosphodiesterase 5 (cGMP-specific) modulates beta-adrenergic signaling in vivo and is down-regulated in heart failure. *Faseb J*. 2001; 15:1718–1726. [PubMed: 11481219]
27. Borlaug BA, Melenovsky V, Marhin T, Fitzgerald P, Kass DA. Sildenafil inhibits beta-adrenergic-stimulated cardiac contractility in humans. *Circulation*. 2005; 112:2642–2649. [PubMed: 16246964]
28. Forfia PR, Lee M, Tunin RS, Mahmud M, Champion HC, Kass DA. Acute phosphodiesterase 5 inhibition mimics hemodynamic effects of B-type natriuretic peptide and potentiates B-type natriuretic peptide effects in failing but not normal canine heart. *J Am Coll Cardiol*. 2007; 49:1079–1088. [PubMed: 17349888]
29. Kuhn M. Structure, regulation, and function of mammalian membrane guanylyl cyclase receptors, with a focus on guanylyl cyclase-A. *Circ Res*. 2003; 93:700–709. [PubMed: 14563709]
30. Feng Q, Lu X, Jones DL, Shen J, Arnold JM. Increased inducible nitric oxide synthase expression contributes to myocardial dysfunction and higher mortality after myocardial infarction in mice. *Circulation*. 2001; 104:700–704. [PubMed: 11489778]
31. Fonarow GC, Abraham WT, Albert NM, Stough WG, Gheorghiade M, Greenberg BH, O'Connor CM, Sun JL, Yancy CW, Young JB. Influence of beta-blocker continuation or withdrawal on outcomes in patients hospitalized with heart failure: findings from the OPTIMIZE-HF program. *J Am Coll Cardiol*. 2008; 52:190–199. [PubMed: 18617067]
32. Lewis GD, Lachmann J, Camuso J, Lepore JJ, Shin J, Martinovic ME, Systrom DM, Bloch KD, Semigran MJ. Sildenafil improves exercise hemodynamics and oxygen uptake in patients with systolic heart failure. *Circulation*. 2007; 115:59–66. [PubMed: 17179022]

### Clinical Perspective

We found that expression of phosphodiesterase 5 (PDE5), an enzyme which hydrolyzes cGMP, was markedly greater in the hearts of patients with end-stage congestive heart failure than in normal (donor) hearts. To ascertain the impact of increased cardiac PDE5 expression on cardiac pathophysiology, we generated mice with cardiac-specific PDE5 overexpression and studied their cardiac structure and function at baseline and after myocardial infarction. Increased cardiac PDE5 levels did not affect baseline cardiac function but predisposed mice to adverse LV remodeling and reduced contractile reserve after MI. Of interest, cGMP levels increased in response to MI in wild-type but not transgenic mice. Our data suggest that increased myocardial cGMP levels constitute an important defense mechanism during combined pressure-volume overload, which acts, in part, by counteracting the effect of unopposed, beta-adrenergic stimulation. This study provides a strong rationale for clinical testing of PDE5 inhibitors or alternative myocardial cGMP-enhancing agents, including soluble guanylate cyclase activators, in patients with congestive heart failure. Additional studies on the extent and temporal distribution of PDE5 expression and myocardial cGMP levels at earlier stages of heart failure are required to determine best conditions for pharmacological intervention.

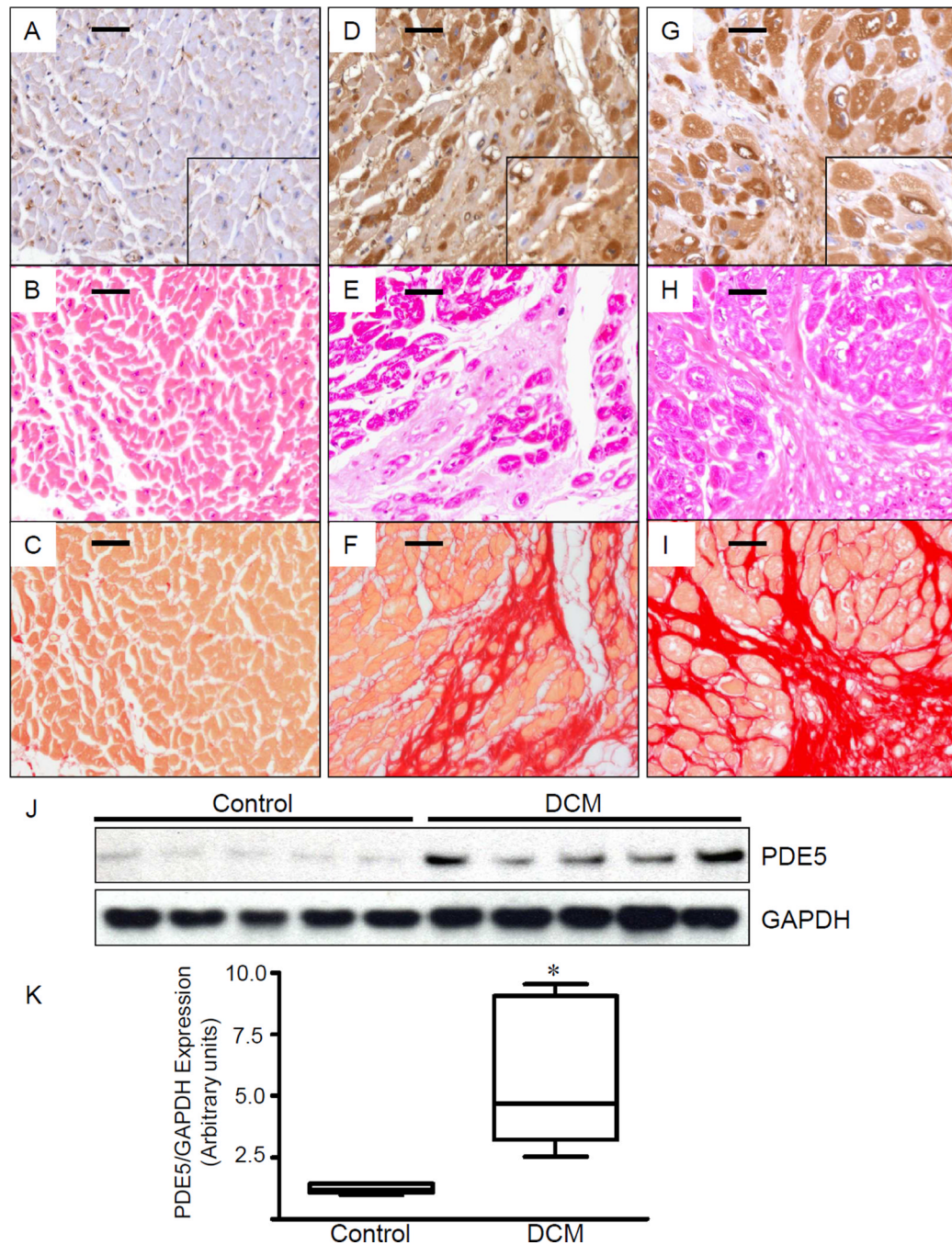


**Figure 1. Left ventricular PDE5 expression is increased in human cardiomyopathies**

Representative examples are shown from control patients (A–C) and patients with dilated (D–F) and ischemic (G–I) cardiomyopathy. Compared to hearts of individuals without cardiac disease (A–C), abundant PDE5 immunoreactivity is present in the LVs of patients with end-stage dilated (D) and ischemic (G) cardiomyopathies. In control heart, PDE5 immunoreactivity is limited and mostly restricted to vascular smooth muscle cells in small and medium-sized arterioles (A, inset). In ischemic cardiomyopathy, PDE immunoreactivity is focal and strongly expressed in residual cardiomyocytes in areas with replacement fibrosis (G, inset). Hematoxylin-eosin staining (B, E and H) and Sirius red staining (C, F and I) delineate preserved cardiac tissue and areas of collagen deposition, respectively.

Immunoblot and densitometric analysis revealed increased PDE5 expression in LVs of patients with dilated cardiomyopathies (J, K).

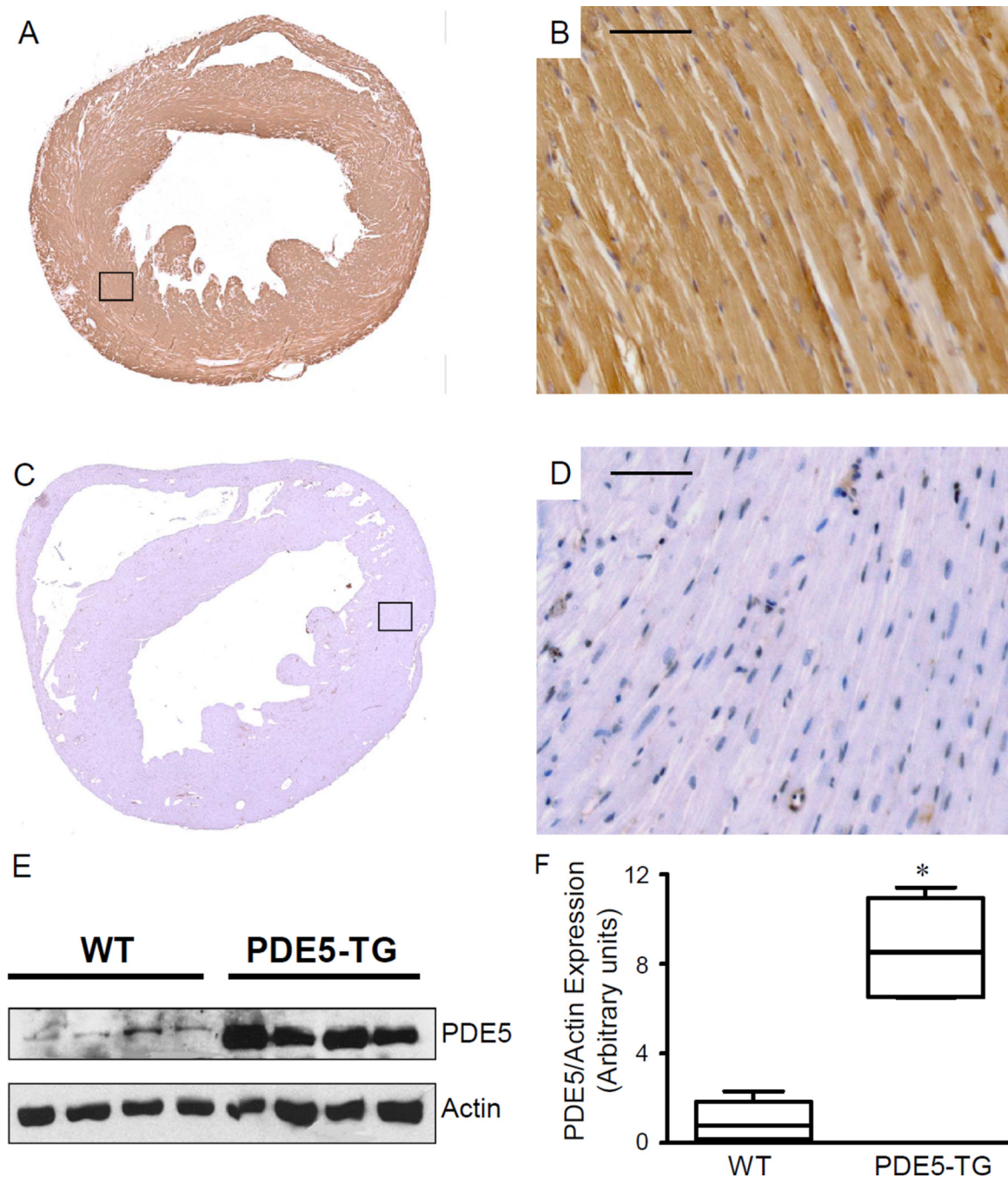


**Figure 2. PDE5 expression is increased in hearts of transgenic mice**  
 Immunohistochemical staining demonstrated abundant PDE5 expression in hearts of PDE5-TG (A, B) compared to WT (C, D). At higher magnification (20x, B, D), moderate PDE5 expression can be observed in the wall of cardiac blood vessels of both genotypes, while abundant PDE5-expression is present in cardiomyocytes of PDE5-TG. Immunoblot and densitometric analysis (E, F) confirmed abundant PDE5 expression in PDE5-TG.

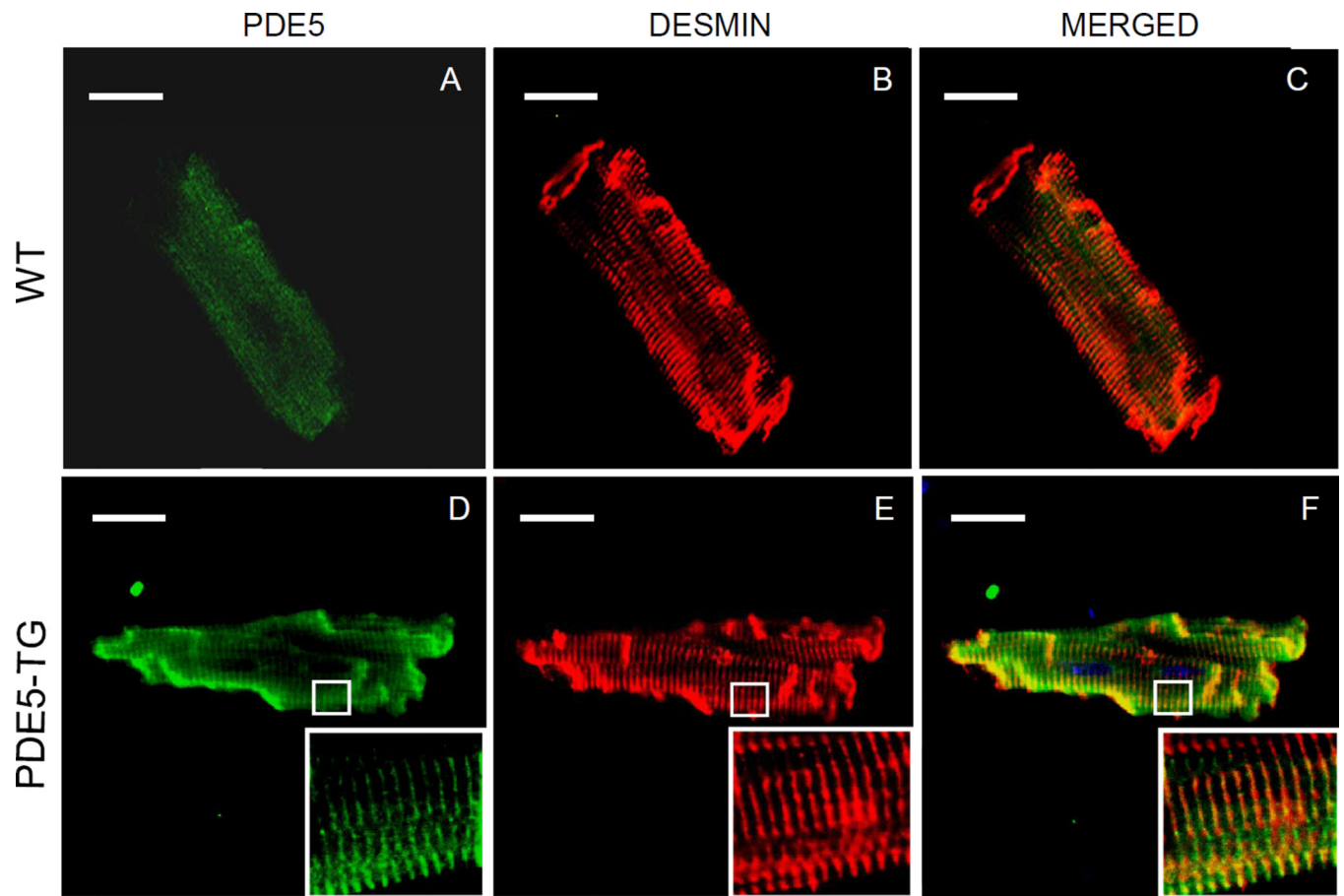


**Figure 3. Localization of PDE5 in cardiomyocytes**

Cardiomyocytes isolated from adult WT (A–C) and PDE5-TG (D–F) mice were stained with fluorescently-labeled secondary antibodies against antibodies recognizing PDE5 (green, A and D) and desmin (red, B and E) and were scanned using confocal laser microscopy. The merged view demonstrates that overexpressed PDE5 was predominantly localized to Z-bands (yellow, C and F). Scale bars indicate 20- $\mu$ m.



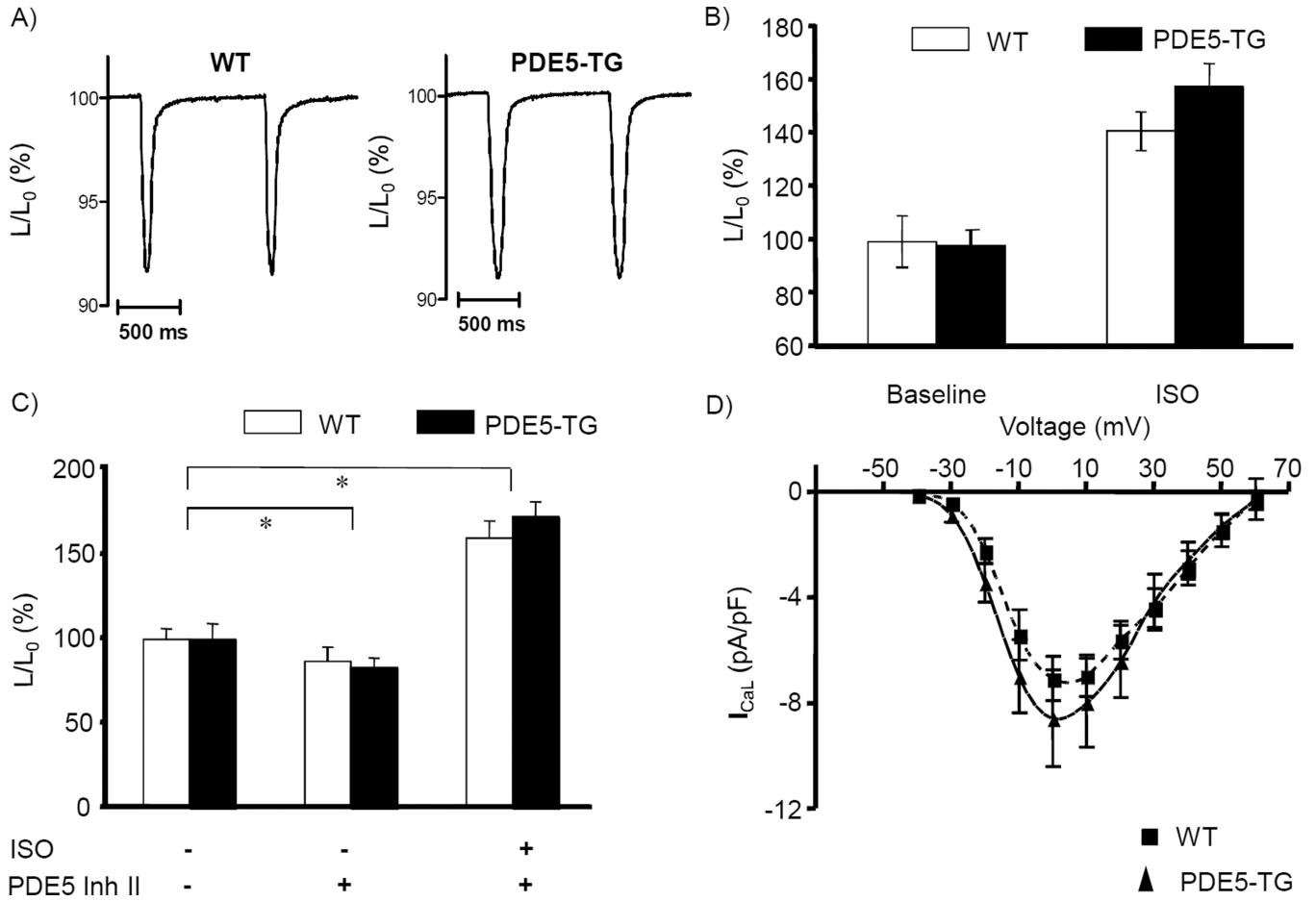


**Figure 4. Contractile function, calcium handling, and electrophysiological properties of isolated cardiomyocytes from WT and PDE5-TG mice**

Examples of cell shortening during 1-Hz field-stimulation confirm comparable fractional shortening normalized to resting cell length,  $L/L_0$ , of paced cardiomyocytes (mean 7.6% in WT versus 7.3% in PDE5-TG, >60 cells per group, A). Contraction, indicated as percent cell shortening, significantly increased following isoproterenol stimulation in both genotypes (n=13 and 16 for WT and PDE5-TG) (B). Following PDE5 inhibition, contraction is modestly reduced compared to baseline and enhanced again after  $\beta$ -adrenergic stimulation; relative changes are similar in WT (n=5) and PDE5-TG cardiomyocytes (n=5) (C). Amplitude and voltage dependence of L-type calcium channel current  $I_{CaL}$  were similar in both genotypes (n=11 WT, n=11 PDE5-TG) (D). \*P<0.05 for the effect of the intervention compared to baseline.

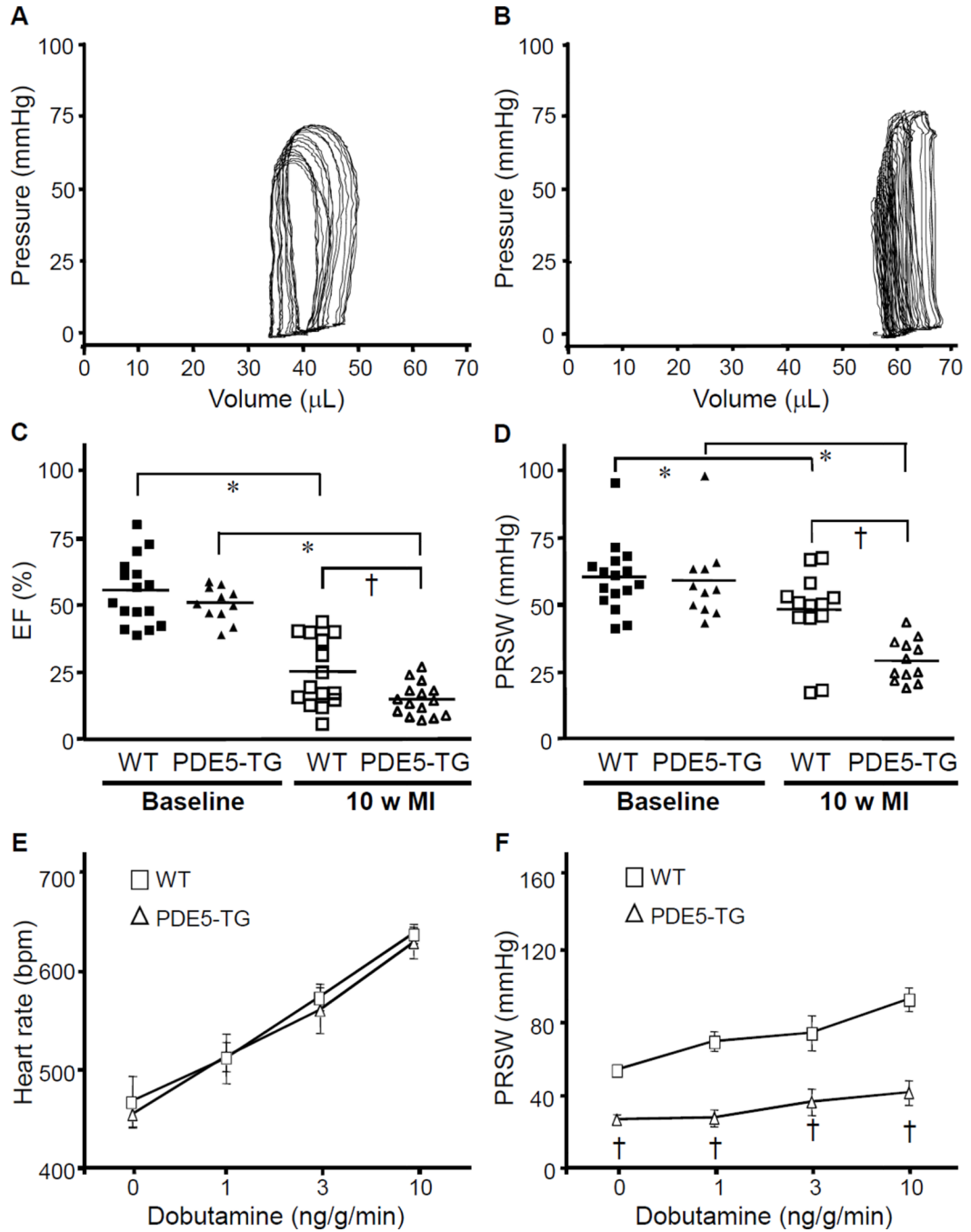


**Figure 5. Hemodynamic measurements at baseline and 10 weeks after MI**  
 Representative pressure-volume loops from WT (A) and PDE5-TG (B) mice 10 weeks after LAD occlusion. Note the rightward shift of the pressure-volume tracings obtained from PDE5-TG. Ejection fraction (C) and preload-recruitable stroke work (D) significantly decreased 10 weeks after MI in both genotypes and to a greater extent in PDE5-TG (\* $P < 0.05$  versus baseline; † $P < 0.05$  versus WT). The dobutamine-induced increase in heart rate was similar in both genotypes (E), whereas the increase in PRSW was blunted in PDE5-TG mice (F). † $P < 0.0001$  versus WT.

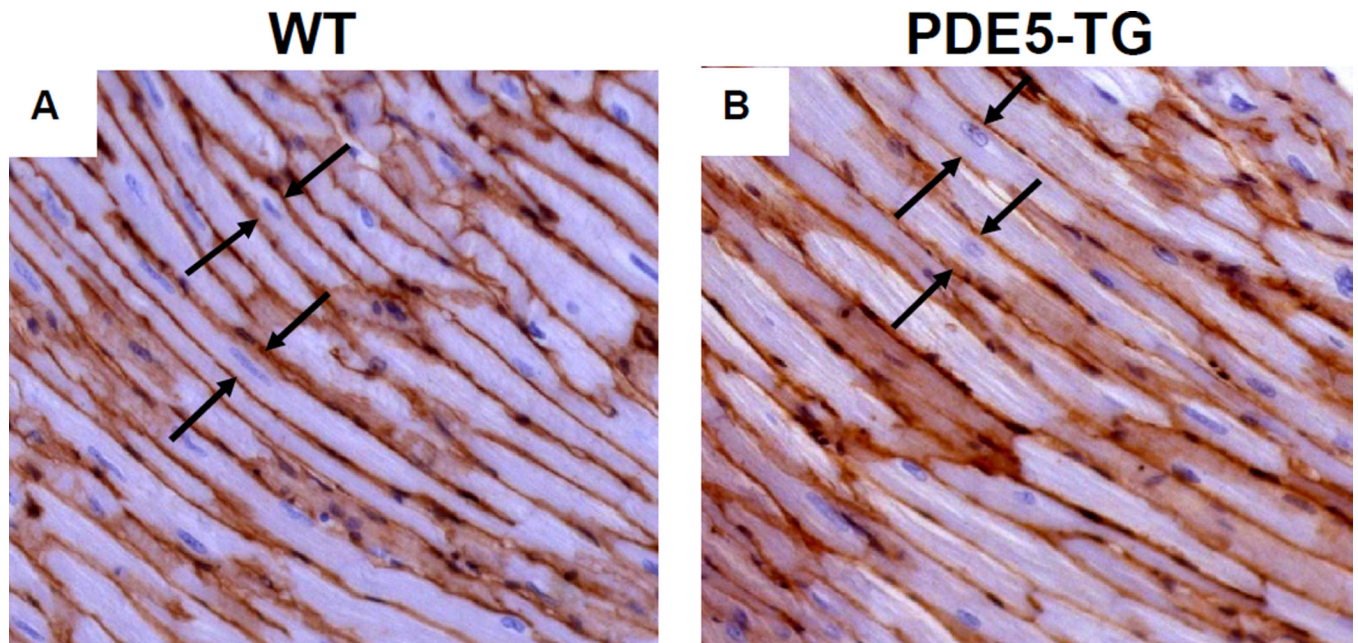


**Figure 6. Cardiomyocyte width in remote myocardium of WT and PDE5-TG at 10 weeks after myocardial infarction**

Representative sections of cardiomyocytes from WT (A) and PDE5-TG (B) mice 10 weeks after MI were stained with laminin, and cell width was measured at the level of the nucleus in longitudinally-sectioned myocytes. Ten weeks after MI, cardiomyocyte width was greater in PDE5-TG than in WT (distance between cell membranes indicated by arrows).

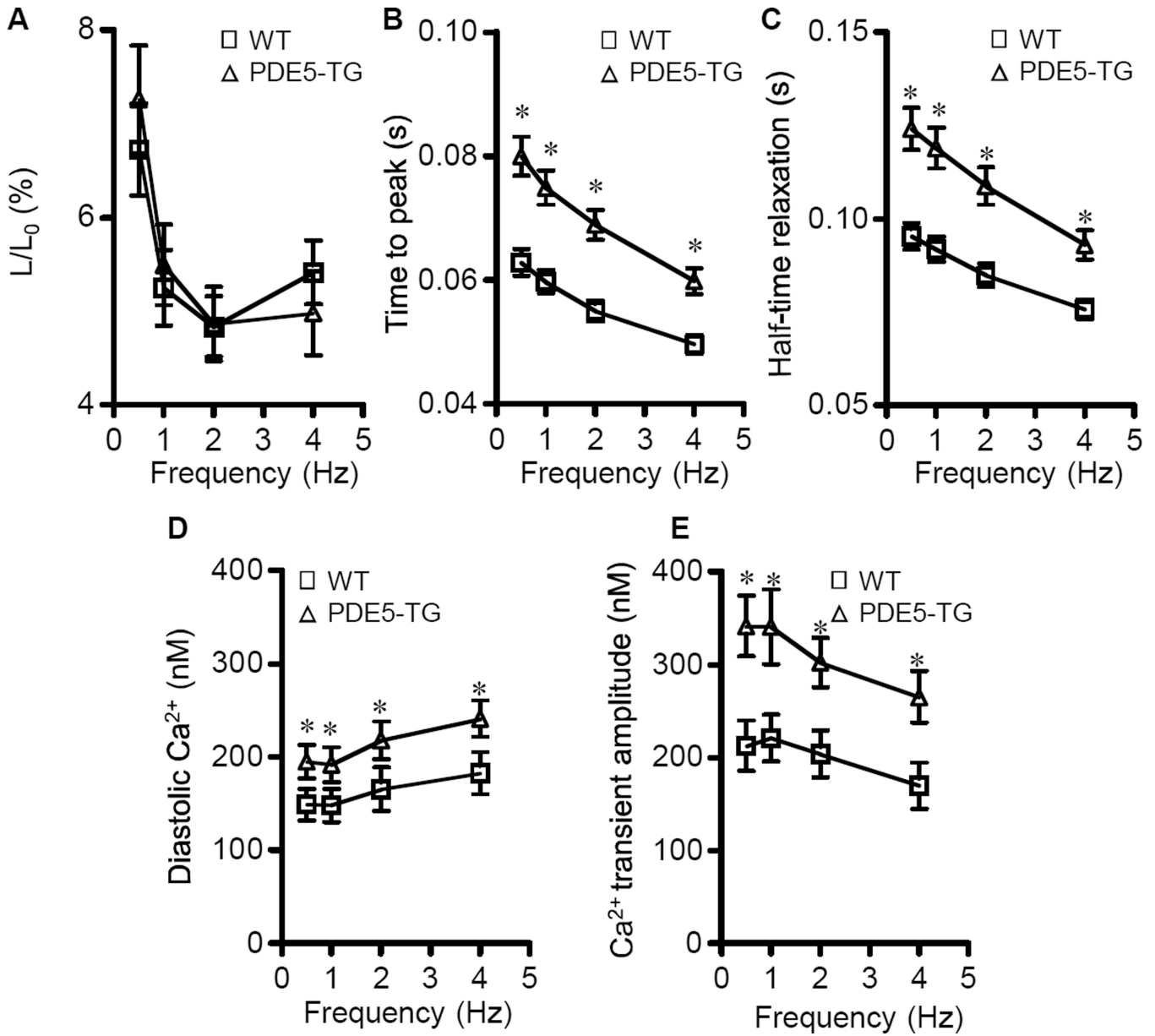


**Figure 7. Unloaded cell shortening, and calcium handling of cardiomyocytes isolated from WT and PDE5-TG at 10 weeks after myocardial infarction**

Unloaded cell shortening ( $L/L_0$ ) at different stimulation frequencies are similar for both genotypes (A), while kinetics of shortening differ significantly with longer time to peak shortening (B) and half-relaxation times (C) in PDE5-TG ( $n=19$  cells) versus WT ( $n=33$  cells). Diastolic resting  $Ca^{2+}$  concentrations (D) and amplitudes of  $Ca^{2+}$  (E) transients are significantly greater in cardiomyocytes isolated from PDE5-TG ( $n=15$  cells) versus WT ( $n=21$  cells). \* $P<0.05$  versus WT.

**Table 1**

Hemodynamic parameters at baseline and 10 weeks after MI.

	Baseline		10 weeks after MI	
	WT	PDE5-TG	WT	PDE5-TG
HR (bpm)	463±12	463±9	475±9	472±14
ESV (μL)	15±2	17±1	39±4 <sup>*</sup>	57±5 <sup>*,†</sup>
EDV (μL)	26±2	29±2	48±4 <sup>*</sup>	65±6 <sup>*,†</sup>
ESP (mmHg)	73±1	79±4	66±2	70±3
EDP (mmHg)	3.5±0.4	3.6±0.6	3.5±0.9	6.5±1.3
CO (mL/min)	6.8±0.4	7.2±0.5	5.3±0.6	4.9±0.8
SW (mmHg·μL)	941±83	1002±89	524±95 <sup>*</sup>	372±86 <sup>*</sup>
Ea (mmHg/μL)	5.3±0.3	5.2±0.3	7.4±1	10.2±3
PAMP (mW/μL <sup>2</sup> )	94±15	84±14	25±5 <sup>*</sup>	13±3 <sup>*</sup>
Tau (ms)	7.3±0.4	7.4±0.4	8.2±0.5	10.4±0.5 <sup>*,†</sup>
Slope of EDPVR	0.26±0.02	0.25±0.03	0.33±0.05	0.70±0.17 <sup>*</sup>

HR, heart rate; ESV and EDV, end-systolic and end-diastolic volume; ESP and EDP, end-systolic and end-diastolic pressure; CO, cardiac output; SW, stroke work; Ea, effective arterial elastance; PAMP, preload-adjusted maximal power; Tau, isovolumic relaxation time (Weiss); Slope of EDPVR, slope of end-diastolic pressure-volume relationship.

\* P<0.05 versus same genotype at baseline,

† P<0.05 versus WT after MI

## 2

## Myocardial remodeling and collagen content 10 weeks after MI.

	WT	PDE5-TG
<b>Heart weight (mg, n=15)</b>	192±9	224±15
<b>HW/BW (mg/g, n=15)</b>	7.0±0.3	8.1±0.4 *
<b>Collagen-type III (% , n=7)</b>	12±2	14±2
<b>Collagen-type I (% , n=7)</b>	6±0.3	5±0.9

HW/BW, heart-to-body weight ratio,

\*  
P<0.05.